Metallothionein-I as a direct link between therapeutic hematopoietic stem/progenitor cells and cerebral protection in stroke

Authors: Helen K. Smith[1,2] PhD, Seiichi Omura[3,4] PhD, Shantel A. Vital[1] MS, Felix Becker[1,5] MD, Elena Y. Senchenkova[1] PhD, Gaganpreet Kaur[1] BSc, Ikuo Tsunoda[3,4,6] MD PhD, Shayn M. Peirce[7] PhD, Felicity N. E. Gavins[1,6] PhD[±]

Affiliations:

[1]Department of Molecular & Cellular Physiology, Louisiana State University Health Sciences Center-Shreveport, Shreveport, LA, USA.

[2]Pathology and Laboratory Medicine, Weill Cornell Medical College, New York City, NY, USA.

[3]Department of Microbiology and Immunology, Louisiana State University Health Sciences Center-Shreveport, Shreveport, LA, USA.

[4]Department of Microbiology, Kindai University Faculty of Medicine, Osakasayama, Osaka, Japan.

[5]Department for General and Visceral Surgery, University Hospital Muenster, Muenster, Germany.

[6]Department of Neurology, Louisiana State University Health Sciences Center-Shreveport, Shreveport, LA, USA.

[7]Department of Biomedical Engineering, The University of Virginia, Charlottesville, VA, USA.

Corresponding author:

Felicity N. E. Gavins, PhD

Department of Molecular & Cellular Physiology

Louisiana State University Health Sciences Center Shreveport

1501 Kings Highway

Shreveport, LA 71103, USA

Tel: +1-318-675-4199

Fax: +1-318-675-6005

Email: fgavin@lsuhsc.edu

Short title: MT-I in HPSC-treatment of cerebral ischemia

Word count: 8766

Non-standard abbreviations: Ischemia-reperfusion injury (I/RI), hematopoietic stem/progenitor cells (HSPCs), hematopoietic SCs (HSCs), ischemic stroke (IS), metallothioneins (MTs), intravital fluorescence microscopy (IVM), middle cerebral artery occlusion and reperfusion (MCAo), lineage negative (Lin-), infarct volume (IV), neurological score (NS), LysM-eGFP (LyZM), enhanced green fluorescent protein (eGFP)

Abstract

Stroke continues to be a leading cause of death and disability worldwide, yet effective treatments are lacking. Previous studies have indicated that stem-cell transplantation could be an effective treatment. However, little is known about the direct impact of transplanted cells on injured brain tissue. We wanted to help fill this knowledge-gap and investigated effects of hematopoietic stem/progenitor cells (HSPCs) on the cerebral microcirculation following ischemia-reperfusion injury (I/RI). Treatment of HSPCs in I/RI for up to 2-weeks post-cerebral I/RI led to: decreased mortality rate, decreased infarct volume, improved functional outcome, reduced microglial activation and reduced cerebral leukocyte adhesion. Confocal microscopy and FACs analyses showed transplanted HSPCs emigrate preferentially into ischemic cortex brain parenchyma. We isolated migrated HSPCs from the brain and using RNA-seq to investigate the transcriptome we found Metallothionein (MT, particularly MT-1) transcripts were dramatically upregulated. Finally, to confirm the significance of MT, we exogenously administered MT-1 following cerebral I/RI and found that it produced neuroprotection in a manner similar to HSPCs treatment. These findings provide novel evidence that the mechanism through which HSPCs promote repair following stroke maybe via direct action of HSPC-derived MT-1 and could therefore be exploited as a useful therapeutic strategy for stroke.

Introduction

The pathophysiology of ischemic stroke (IS) is prolonged throughout reperfusion of blood to injured brain tissue (1) through a process known as ischemia/reperfusion injury (I/RI). Although exact mechanisms responsible for post-ischemic cerebral damage are unclear, the inflammation following I/RI could be a contributing factor (2). This injurious process occurs over hours and days subsequent to stroke onset and thus provides an extended window for intervention beyond excitotoxic cell death, initiating within just minutes.

Experimentally, stem cell (SC) treatments for IS have shown great success by improving both survival and functional recovery (3-5). These results have been observed after administration of SCs from various lineages: most frequently adipose and other mesenchymal SCs (6, 7), neural SCs (8), and hematopoietic SCs (HSCs) (9), as-well-as after administration of induced pluripotent SCs that were reverse-engineered from fibroblasts (10) (embryonic or fetal SCs are now rarely used (3)).

Clinically, trials are tentatively progressing on a large body of data reporting the secondary effects of SCs that is rarely underpinned by evidence of direct mechanisms through which SCs elicit protection. Recently, CD34$^+$ HSCs successfully passed a Phase I clinical trial that assessed the safety and feasibility of the treatment (11). Patients in this trial had reduced brain lesions at the 6-month endpoint of the study and showed no significant treatment-related adverse effects. Despite its success this trial and the majority of related studies have not demonstrated how transplanted cells are directly of benefit to injured brain tissue, thus preventing optimization of the therapy (12).

Several lines of evidence indicate the anti-inflammatory nature of transplanted SCs: SC treatment appears to correlate with increased anti-inflammatory interleukin (IL)-10 and transforming growth factor beta (TGFβ), as opposed to pro-inflammatory IL-1β and tumor necrosis factor alpha (TNFα) (13). In addition, some evidence indicates the ability of SCs to promote growth and survival of surrounding tissue via secretion of vascular endothelial growth factor (VEGF) (14) or other growth factors (15). Despite these findings,

treatment with these elements individually is not able to replicate the success of SCs to any significant degree in clinical trials. Gaining further insight into mechanisms of SC therapy, as well as improving the migratory properties of transplanted cells, will provide huge potential for optimizing their use. It may also pave the way for their replacement with pharmaceuticals (16). Although autologous bone marrow-derived cells form the patients would remain the optimal option, the current practice of harvesting an autologous population of cells from the bone marrow of patients following stroke is both time and cost ineffective and involves subjecting frail stroke patients to an invasive surgical procedure.

Populations of lineage negative (Lin-) hematopoietic stem/progenitor cells (HSPCs) were assessed for their potential in limiting brain damage following cerebral I/RI. We demonstrated a novel role of murine HSPCs in regulating leukocyte-endothelial interactions in the cerebral microvasculature following I/R, coupled with decreasing mortality, infarct volume (IV) and neurological score (NS) when administered as late as 24-h after stroke. The HSPCs migrated readily and without co-treatment with migration-enhancing cytokines such as granulocyte macrophage colony-stimulating factor [GM-CSF]. We also demonstrated increased levels of metallothioneins (MTs, low molecular weight anti-oxidative proteins) transcripts, especially MT-1 in explanted HSPCs as determined using RNA sequencing (RNA-seq) analysis. Lastly, treatment of mice with MT-1 significantly reduced IV and NS. Our studies could further advance HSPCs as a promising therapeutic strategy for promoting repair in cerebral I/RI.

Materials and Methods

All studies were done blinded and performed on adult male mice. Wild-type (WT) C57BL/6 mice weighing 25-29g were purchased from Jackson Laboratory (Bar Harbor, ME, USA). C57BL/6 LysM-eGFP (LyZM) mouse strain (constitutively expressing green fluorescent protein (eGFP) in myeloid cells) weighing 15-17g (4-5-wk-old) were a generous gift from Dr. Paul Kubes (University of Calgary, AB, Canada) and bred on site. Mice were maintained on a 12-h light-dark cycle during which room temperature (RT) was maintained at 21-23°C, and had access to a standard chow pellet diet and tap water *ad libitum*. All animal experiments were approved by the Louisiana State University Health Sciences Center-Shreveport (LSUHSC-S) Institutional Animal Care and Use Committee (IACUC) and were in accordance with the guidelines of the American Physiological Society.

Middle cerebral artery occlusion and reperfusion (MCAo)

As a cerebral I/R model, MCAo was performed as previously reported (17) Briefly, mice were anaesthetized with i.p. injection of ketamine (150mg/kg) and xylazine (7.5mg/kg) and MCA was occluded for 30-min using a 6-nylon intraluminal filament (Doccol Corporation, Sharon, MA, USA), followed by 24-h, 48-h, 1-wk or 2-wk reperfusion. Sham-operated mice were subject to anesthesia and other surgical procedures without MCA occlusion.

Cerebral intravital fluorescence microscopy (IVM)

IVM was performed as previously described (2). Briefly, mice were re-anaesthetized with i.p. injection of ketamine (150mg/kg) and xylazine (7.5mg/kg). The jugular artery and vein were cannulated to monitor mean arterial blood pressure (MABP), as well as for i.v. administration of rhodamine 6G. The head of each mouse was fixed in a frame in sphinx position and left parietal bone exposed by a midline skin incision, followed by a craniectomy (diameter: 2.5mm). A 12mm glass coverslip was placed over the craniectomy and the space between the glass and the dura mater was filled with artificial cerebrospinal fluid (aCSF; Na^+ 147.8mEq/L, K^+ 3.0mEq/L, Mg^{2+} 2.3mEq/L, Ca^{2+} 2.3mEq/L, Cl^- 135.2mEq/L, HCO_3^- 19.6mEq/L, lactate$^-$ 1.67mEq/L, phosphate 1.1mM, and glucose 3.9mM; all Sigma-Aldrich, ST Louis, MO, USA). A Zeiss

Axioskop microscope (Zeiss, Thornwood, NY, USA) with a mercury lamp was used to observe the pial venules in the cerebral cortex. Two-minute videos were captured with a CoolSNAP HQ[2] (Photomerics, Tuscon, AZ, USA) black-and-white camera and recorded for offline analysis.

Confocal IVM

MCAo was performed as described above in LyZM mice. 24-h into reperfusion, mice were treated with Cell Tracker Red labelled-HSPCs. 24-h after treatment (48-h after MCAo), mice were placed on an Olympus BX51WI upright microscope (Olympus, Venter Valley, PA, USA) with a 20X (LUCPlanFLN) objective and equipped with a 3i LaserStack laser launch (3i, Denver, CO, USA), Yokogawa CSU-X1-A1N-E spinning disk confocal unit (Yokogawa Electric Corporation, Tokyo, Japan) and electron multiplier CCD camera (C9100-13, Hamamatsu, Bridgewater, NJ, USA). Mice were treated with platelet-endothelial cell adhesion molecule (PECAM)-1] antibody (viewed at 594nm, 20μg per mouse, i.v. (eBioscience, CA, USA)) to visualize vessels.

Video analysis for IVM studies

Three to five randomly selected vessels, 30–70μm in diameter and 100μm long, were observed for each mouse after treatment. Adherent leukocytes were defined as cells remaining stationary for ≥30 seconds (s), expressed as the number of cells per square millimeter of the vessel surface and calculated from diameter and length, assuming cylindrical shape.[2]

Infarct volume (IV)

After a 24-h reperfusion period, mice were euthanized and brains removed and placed into 4°C phosphate-buffered saline (PBS, Sigma-Aldrich) for 15-min; sectioned (2mm) and stained with 2% 2,3,5-triphenyltetrazolium chloride (TTC) in PBS at 37°C for 15-min and fixed by immersion in 10% formaldehyde. Stained sections were photographed and the digitized images of each brain section (and the infarcted area) were quantified using a computerized image analysis program (NIH 1.57 Image Software).

Mortality rate

Mortality rate was a binary evaluation, calculated as the percentage of animals alive in each group post-MCAo (24-h after treatment with either HPSCs or vehicle, see below for treatment details).

Neurological score (NS)

The functional consequences of cerebral I/R injury were evaluated by assessing general, sensory, motor and proprioceptive deficits that were assessed in a blinded fashion (Table 1). The 18-point score was compiled from a previously published scoring system to provide objective ('yes or no') criteria for assessment (18, 19). A maximal score of 18 could be assigned to each experimental animal.

Blood and tissue collection

Blood was taken by cardiac puncture and centrifuged at 4°C, 450g for 5-min to yield plasma. Brains were dissected out and either snap frozen in liquid nitrogen or perfused with 10ml saline followed by 10ml 4% paraformaldehyde, then transferred into increasing concentrations of sucrose (20-30%) over 4 days. Fixed tissue was cryopreserved in Optimal Cutting Temperature compound (Thermo Fisher Scientific, NC, USA), then both sets of samples were stored at -80 °C until required.

Bone marrow extraction

4-5-wk old male mice (15-17g) were euthanized and femurs and tibias removed. Bones were flushed through with sterile Hank's Buffered Saline Solution using a 25G needle. BM was dissociated mechanically, filtered through a 70μm gauze, centrifuged for 10-min at 450g, resuspended in 10ml PBS then counted using a cell counter (Thermo Fisher Scientific).

Selection of HSPCs

After BMCs were extracted, Lin⁻ cells were negatively selected using magnetic beads, according to the manufacturer's instructions of a hematopoietic cell selection kit (Stem Cell Technologies Ltd, BC, Canada). The lineage cocktail used to removed unwanted/differentiated cells consisted of: CD45R (B cells), CD11b

(granulocytes, macrophages, and natural killer cells), CD3e (T cells), Ly-6G (lymphocytes), TER119 (erythrocytes).

Labelling HSPCs with carboxyfluorescein succinimidyl ester (CFSE)

HSPCs were reconstituted at $1x10^6$ cells in 0.1% BSA, and incubated with 2µl of 5mM CFSE/ml cells at 37°C for 10-min. Following incubation, cells were washed three times by centrifuging for 10-min at 450g and reconstituted at the required concentration (see below) in PBS. After staining, cell viability was 99-100%, as observed with trypan blue staining.

Labelling HSPCs with Cell Tracker Red

HSPCs were reconstituted 5 x 10^6 cells/ml in PBS. Cell Tracker Red dye (ThermoFisher, Waltham, MA) was added to make a final concentration of 5 µM at 37°C for 10-min (20). Following incubation, cells were washed three times by centrifuging for 10-min at 450g and reconstituted at the required concentration (see below) in PBS. After staining, cell viability was 99-100%, as observed with trypan blue staining.

Administration of HSPCs

Under isoflurane anesthesia, mice injected i.v. with either $1x10^6$ cells in 100µl PBS, $1x10^7$ cells in 200µl PBS, or vehicle (PBS). Cell viability was checked using trypan blue stain prior to injection (viability = 98-100%), and care was taken to dissociate cells thoroughly prior to administration. All experiments were double-blinded, whereby the investigator administering treatments was unaware of the treatment type (HSPCs or vehicle), and an investigator unaware of the treatment mice conducted assessments of mice both pre- and post-mortem.

Treatment with metallothionein I (MT-I) Mice were subjected cerebral I/R (30-min ischemia followed by 48-h reperfusion) and treated with metallothionein (MT)-I, i.p. 5µg/g body weight (21) (Enzo Life Sciences, NY, USA) at the start of reperfusion. Control mice were injected with PBS.

Imunohistochemistry (1) Immunofluorescence staining for neuroinflammation

Cryopreserved brains were sectioned (18μm) and stained for activated microglia. Non-specific binding sites were blocked with 10% normal serum (Vector Laboratories, Burlingame, CA, USA) for 1h at RT. Sections were incubated with primary antibodies (diluted in 10% normal serum in PBS) at 4°C overnight. Microglia were detected by anti-Iba-1 antibody (Wako, Richmond, VA, USA, 1:1000). Secondary antibody used was goat anti-rabbit IgG (Life Technologies, CA, USA) for 1-h at RT, Alexa Fluor 488 (Vector Laboratories) for 30-min at RT.

Immunohistochemistry (2) 3,3'-Diaminobenzidine DAB staining for localized CFSE-positive HSPCs

DAB staining was used to identify localized CFSE-positive (HSPC) cells. Slices were rinsed in PBS and covered with 0.5% fish serum gelatin (FSG) in PBS for 5-min. The FSG was aspirated and incubated with a HRP-conjugated anti-fluorescein antibody (Abcam, Cambridge, MA, USA) 1:200, for 1-h. The antibody was washed (three times) with PBS and slide incubated with 0.05% DAB and 0.015% H_2O_2 for 5-min, then counter-stained with hematoxylin.

FACS analysis of stem cell markers and cell sorting of CFSE-positive cells from whole brain

Analysis of CD34, Sca-1, c-kit, CD31-positive cells was performed on an LSRII flow cytometer (BD Biosciences, San Jose, CA, USA) and CFSE+ cells were sorted on a FacsAriaIII (BD Biosciences). Where FACS sorting was used to retrieve CFSE-positive transplanted HSPCs, experiments were conducted 24-h after administration of HSPCs, in order to ensure cells had time to migrate into the brain.

Western Blotting

Total protein was extracted in RIPA buffer (Sigma-Aldrich) by homogenization and sonication. Sonication followed by centrifugation at 2000g for 15-min at 4^0C was repeated till clear solution was obtained. The concentration of protein in lysate was measured by Pierce^{TM} BCA Protein Assay Kit (Thermo Fisher Scientific). 30μg of protein was mixed with loading buffer (2X Laemmli Buffer (Bio-Rad, CA, USA)). The mix was loaded on 12% SDS-polyacrylamide gel with the appropriate molecular weight markers and

transferred to polyvinylidene fluoride (PDVF) membranes. Reversible protein staining of the membranes with 0.1% Ponceau S in 5% acetic acid was used to verify even protein transfer. Membranes were blocked with 5% non-fat dry milk followed by overnight incubation with 2μg/ml MT-1 primary antibody (Biomatik, Delaware, USA). This was followed by 30-min washing with Tris-buffer saline containing Tween-20 and incubation for 60-min at RT with diluted horseradish peroxidase-conjugated secondary antibody (1:2500. Sigma- Aldrich). Membranes were washed for 30 min and proteins detected by ECL detection kit (Bio-Rad) using film (Bio-Rad). Stripping was done using Re-blot Plus (EMD Millipore, MA, USA) and blocked with 5% non- fat dry milk. Membranes were incubated for 60-min at RT with 1:2000 diluted beta-tubulin primary antibody and suitable secondary antibody (Cell Signaling, MA, USA). Relative band intensity was quantified using NIH image software 1.63.

RNA sequencing (RNA-seq)

RNA library preparation, sequencing reactions, alignment, and read count were conducted at GENEWIZ, LLC. (South Plainfield, NJ, USA). Briefly, cDNA was directly synthesized from cell lysate and amplified by PCR, using SMARTer Ultra Low Input RNA kit for sequencing-v3 (Clontech Laboratories, Mountain View, CA, USA). The Illumina Nextera XT DNA sample Prep Kit (Illumina, San Diego, CA, USA) was used to generate sequencing libraries from the cDNA. Sequencing libraries were validated, using the Agilent 2100 Bioanalyzer (Agilent Technologies, Santa Clara, CA, USA), and quantified, using Qubit 2.0 Fluorometer (Invitrogen, Gran Island, NY, USA) as well as real-time PCR (Applied Biosystems, Foster city, CA, USA). Sequencing libraries were sequenced on the Illumina HiSeq 2500, according to manufacturer's instruction. Sequencing was performed, using a 1x50 Single Read configuration. The raw sequences obtained were subject to quality trim and adaptor removal, using trimmomatic-0.32. Within the CLCbio software environment (CLC genomics workbench 8.0.3, CLC Genomics Server 7.0.3), the trimmed sequences were aligned to reference genome, Mus musculus GRCm38.75, downloaded from ENSEMBLE (http://www.ensembl.org/). RNA sequencing data have been deposited into the Gene Expression Omnibus (GEO) in National Center for Biotechnology Information (NCBI). Accession number: GSE95853.

RNA-seq data analyses

Exon read count data of 12 samples given by the company were normalized with two methods: 1) read counts per kilobase (RPK) and 2) tag count comparison (TCC), using "R" (22). RPK was conducted to compare the read count data among the different genes in each sample by normalizing to read counts per kilobase exon length (23), while TCC was conducted to compare the read count data among the 12 samples by normalizing whole read count data, using read counts of non-differentially expressed genes (24).

Volcano plot

A volcano plot was drawn using the OriginPro 8.1 (OriginLab Corporation, MA, USA) to visualize statistical significance together with log ratio of transcriptome data (25). Log ratios of gene expression in treated samples compared with controls were used as the x-axis and the logarithms of p values to base 10 were used as the y-axis.

Functional clustering

To determine what kinds of genes were differentially expressed, we entered a list of genes that were differentially expressed ($p<0.05$, more than 2-fold up or downregulated between the control and treated groups) for the Database for Annotation, Visualization and Integrated Discovery (DAVID; https://david.ncifcrf.gov/). Enrichment score was calculated by Fisher's Exact Test based on number of differentially expressed genes in the sample, matching with the total number of genes that are included in each canonical pathway in the database.

Principal component analysis (PCA)

PCA can reduce the dimensionality of a data set (e.g. RNA-seq data) consisting of a large number of interrelated variables, while retaining as much as possible of the variation present in the data set (26). PCA was conducted as an "unsupervised" analysis to clarify the variance among RNA-seq data among the samples, using a Q-mode PCA package 'prcomp' of R (24). The proportion of variance and factor loading were also calculated (27, 28).

Statistical analysis

Data were analyzed using Student's t-test (two groups), ANOVA with Bonferroni post-tests (more than two groups), or by chi-square analysis (neurological score only). Analysis was performed using GraphPad Prism5 software. Data are shown as mean values ± standard error of the mean (SEM). Differences were considered statistically significant at a value of $p<0.05$.

Results

Freshly harvested HPSCs are a phenotypically stable source of SCs

While CD34 is an established marker of undifferentiated BMCs in humans, in mice, undifferentiated BMCs express CD34 only in low amounts until they are 5-wk-old and cease to express CD34 after 10-wk (29). Thus, we harvested BMCs from 4-5-wk old mice and – rather than CD34-positive selection – used negative selection to isolate the lineage marker-negative (Lin⁻) population of progenitors from whole BM. These cells were phenotypically highly consistent-and were therefore selected for use in this study (Figure 2A).

HPSCs afford protection for up to 2-wk following I/R-induced cerebrovascular injury

Mortality rates following 30-min MCAo and 48-h reperfusion showed HPSCs-treated mice to be protected against I/RI (Figure 2B): the incidences of death 24-h post treatment (48-h reperfusion) in saline-treated control animals and HPSCs-treated mice were 50% and 7%, respectively. No further mortality was observed in either group after 48-h up until 2 wk post-ischemia, the termination of the experiment.

IV of saline-treated or HPSCs-treated mice subjected to 30-min MCAo and 24-h, 48-h, 1-wk or 2-wk reperfusion are presented in Figure 2C and D. Saline-treated mice displayed larger IVs than HPSCs-treated mice at all time points (Figure 2C). At 48-h post MCAo (24-h after treatment), IV in HPSCs-treated mice were reduced by 50% vs. saline-treated mice (10% vs. 27% respectively). Furthermore at 1-wk, no infarct was visible following HPSCs-treatment, whereas saline-treated mice retained infarcts of equivalent volumes (22%) to untreated mice 24-h after MCAo (20%).

HPSCs improve neurological function up to 1 week post cerebral I/RI

We evaluated neurological function in animals after cerebral I/RI using an 18-point NS, which assessed various aspects of functional recovery, including changes in sensory, motor and proprioceptive function in a blinded and binary fashion (Table 1) (18, 19, 30). NS reached 13-, 24-h after stroke (mice with a score 16+ accounted for 90% of the mortality rate). Mice treated with HPSCs showed 50% reduction in NS (on a scale of 0-18, 0 representing no signs of stroke) at 48-h ($p < 0.05$), and 10% in saline-treatment groups (Figure 2).

Furthermore, at 1-wk, HPSCs-treated mice exhibited near sham-level NS, compared with saline-treated mice. All mice were almost fully recovered at 2-wk – the only consistent sign of I/RI (in both groups) being a persistent head tilt more than 10 degrees from the vertical axis, indicating some prolonged motor dysfunction.

Transplanted HPSCs home to the ischemic cortex following cerebral I/RI

To determine whether HPSCs homed to the injured brain in HPSCs-treated mice, we detected CSFE-labelled HPSCs in the ipsilateral hemispheres, indicating localization of HPSCs to the peri-infarct region (Figure 3D). No positive staining was observed in the liver, lung, spleen or muscle (gastrocnemius) (data not shown), indicating that transplanted cells home to the infarcted region. To determine whether transplanted cells had emigrated into the parenchyma (rather than remain adhered to the luminal endothelia), we used confocal IVM to identify fluorescently-labelled HPSCs that had migrated into the brain parenchyma. LyZM mice subjected to 30-min MCAo and 48-h reperfusion (and at 24-h treated with saline or HPSCs stained with Cell Tracker Red) (Figure 3G, Movie 1). HPSCs were detected outside of blood vessels in the cerebral vasculature, while eGFP positive endogenous PMNs were detected inside of blood vessels. At this time point (possibly due to HSPCs having already emigrated), interactions between HSPCs and PMNs were not observed. In addition, we also corroborated both the above findings in FACS sorting experiments designed to extract transplanted cells from the brains of HPSCs-treated mice, thereby identifying the migratory preference of HSPCs towards either the ipsi- or contralateral cerebral hemisphere. This confirmed that CFSE-labelled HPSCs migrated to the ipsilateral versus contralateral hemisphere at a ratio of 10:1 (Figure 3F).

HSPCs reduce cellular responses for up to 1-wk in the cerebral microcirculation of mice following I/R.

Leukocyte-endothelial interactions are required for immune cell infiltration following cerebral I/RI, with high levels of interactions leading to parenchymal inflammation and correlating with poor outcome. To investigate the impact by HPSCs treatment on these interactions, IVM of cortical venules of the ipsilateral

cortex was used to film the interactions in real-time (Figure 4A). In accordance with our previous findings [1,2], MCAo for 30-min followed by 24-h reperfusion induced interactions within the cerebral microcirculation of mice compared with sham animals (Figure 4C, D). Mice treated with HPSCs displayed reduced leukocyte rolling, increased velocity and decreased adhesion at 48h vs. saline-treated mice, whose interactions continued for a further wk (Figure 4). By 2-wk, both saline-treated and HPSCs-treated mice displayed similar effects to pre-stroke levels.

HPSCs protect against augmented neuroinflammation following I/RI

To investigate whether HPSCs could affect neuroinflammation, we monitored microglial activation in saline-treated and HPSCs-treated mice. At 48-h reperfusion, using Iba-1 staining (Figure 5), as expected, Iba-1 expression was substantially elevated in both the ipsilateral (injured) and contralateral side in mice after I/R, with greater expression in the ipsilateral side. Furthermore, when compared with saline-treated mice, HPSCs-treated mice showed a significant decrease in Iba-1 expression, indicating a reduction in microglia activation. No Iba-1 expression was found in sham mice, or sham mice treated with HPSCs (data not shown).

Explanted HPSCs display regulation of MT-I gene profile

To identify potential mechanisms through which HSPCs might directly affect their milieu once transplanted and migrated, we determined the transcriptome profile of HPSCs extracted from the brain following their transplantation 24-h previously, following I/RI. Analysis of transcriptomes showed that 562 genes and 47 genes were significantly up- or downregulated more than 2-fold, respectively, in isolated versus naïve HPSCs (Supplemental Figure 1+Table 1). Among the differentially expressed genes, we examined the expression levels of genes associated with inflammation and angiogenesis (Supplemental Table 2), in which IL-10 receptor α subunit (*Il10ra*) and epiregulin (*Ereg*) were significantly upregulated (*Il10ra*: 4.2-fold, $p < 0.05$; *Ereg*: 6.9-fold, $p < 0.05$), respectively.

To identify molecular pathways that are potentially associated with HSPC activity following their homing to injured tissue, we performed functional clustering, using DAVID (Supplemental Table 3). Among the pathways, the DENN (Differentially Expressed in Normal and Neoplastic cells) domain-related pathway, oligoadenylate synthetase-related pathway, and steroid hormone receptor signaling pathway were listed as top three pathways based on enrichment scores.

We conducted PCA to see overall gene expression patterns among the samples. Principal component (PC) 2, but not PC1, separated samples between controls and treated groups except one sample (sample T12) (Figure 6A). Factor loadings for PC2 showed that upregulation of several genes contributed to the PC2 value positively, while contribution by downregulated genes to the PC2 value was negligible (Figure 6B and Supplemental Figure 1). The factor loadings in PCA are the correlation coefficients (r) between the variables (read numbers of molecules) and factors (PC2 values); the squared factor loadings (r^2) are the amount of explained variation. Among the genes that positively contributed to the PC2 value, only the metallothionein (Mt) 1 gene had moderately high r^2 (=0.38), while the top 10 genes, including other MT genes (*Mt2*, *Mt3*, and *Mt4*), MTa genes (*Mta1*, *Mta2*, and *Mta3*) and other genes (Figure 6B) had low r^2 (<0.2). Based on these findings, we decided to investigate the role of MT-1.

MT-1 attenuates I/R-induced cerebrovascular injury

MT-1 has been shown to be a secreted protein (31). Having demonstrated that explanted HPSCs possess high levels of MT-1 when in the post-I/RI cerebral environment, we ascertained whether protein levels of MT-1 are upregulated in the contralateral and ipsilateral cerebral regions following HSPC administration. Supplemental Figure 2 shows that the expression of MT-1 is upregulated in ipsilateral cerebral regions following HSPC administration, versus vehicle administration. To further build on these findings, we next tested the potential of MT-1 treatment to afford protection following cerebral I/RI. Treatment of mice with MT-1 markedly attenuated the inflammatory response vs. saline-treated mice, as assessed by NS (reduced from 10-12 to 0-3 over 48-h) and IV (Figure 6C-E).

Discussion

This study presents several key novel findings regarding the administration of HSPCs to mice following cerebral I/RI. We demonstrate that: 1) HSPCs mobilize and home to the injured brain without pharmacological intervention, 2) HSPCs exert protection within the cerebral microvasculature and recovery of neurological function, 3) HSPCs emigrate into the brain parenchyma where they produce MT mRNA and furthermore, 4) the protective effects of HSPCs in stroke can be recapitulated by the administration of MT-1 (Figures 6 C-E, 7).

Among the many potential regenerative medicine strategies tailored towards cerebral injury repair, SC-based therapeutics have shown the most promise. Despite the encouraging results suggesting SC therapy, including CD34$^+$ SC, as a stroke treatment, mechanisms of action warrant additional investigations. Endogenous CD34$^+$ SCs are mobilized into the peripheral blood following stroke (32), and enhancing their migration using GM-CSF is highly neuroprotective (33). Results observed in a Phase I trial treating five ischemic stroke patients with 1×10^8 CD34$^+$ HPSCs indicated that transplantation of these cells might also induce neuroprotection, although mechanism of action remained unknown. We demonstrate herein that mice treated with HSPCs displayed an abrogated neuroinflammation with neuroprotection following I/RI. This was observed by decreased adherent leukocytes, which is consistent with the cerebral effects observed in other models (e.g. systemic administration of lipopolysaccharide (34)), and decreased microglial activation, along with decreased IV (which has been linked to levels of inflammation during cerebral reperfusion), decreased NS and increased survival. Our results are in-line with experimental and clinical findings supporting the use of SCs as a therapeutic in ischemic stroke. Furthermore, here we show that HPSCs may be a promising source of therapeutic SCs, supported by our findings that the injected HPSCs mobilized and preferentially homed to the ischemic hemisphere following cerebral I/R.

Route of administration of SCs for treatment has long been under debate. Recent studies have shown that there is little or no difference in benefit between cells administered either i.v. or i.a. (35), Thus, we chose to administer 1×10^6 (within the range of HSC numbers that have been used in previous publications, from

5x10^5 (34), to 8x10^6 (37)) HPSCs i.v. (by using a venular access point for the treatment rather than the carotid artery, patients need not be excluded based on carotid stenosis). In addition, we administered HPSCs 24-h after stroke to represent a treatment regimen which can be applied to patients (i.e. after the onset of stroke) (38), in contrast to previous "prophylactic" studies that – while demonstrating efficacy of CD34$^+$ HSC – administered cells as early as 48-h prior to stroke (36).

In this study, although HPSCs were found to be present in both the contralateral and ipsilateral (infarcted) hemispheres, considerably greater numbers were found in the ipsilateral hemisphere of experimental mice. Differences in the integrity and pathophysiological status of the blood-brain barrier (2) may facilitate HSPCs into the ischemic hemisphere more selectively (39), while some studies have shown that cells fail to localize to an infarct at all (although in some cases are still protective) (40).

In addition, with respect to HSPC migration, we were able to achieve efficient migration when administering cells i.v. Clinical trials have commonly opted for i.a. administration via the common carotid artery ipsilateral to the infarct, since intuitively it is the most efficient way to deliver the largest number of cells rapidly to the infarct area, while avoiding the considerable invasiveness of i.c.v. injection. Pre-clinically, recent work has shown little or no improvement when using i.a. and i.c.v. approaches compared with i.v. (41), with cells able to migrate in significant numbers to an infarct region having been administered i.v. (although some studies describe large numbers of cells becoming lodged in the lungs (40, 42)). This less-invasive route is preferable in a clinical setting when dealing with patients who are both frail and immunocompromised following stroke. Moreover, i.a. administration may be additionally deleterious due to the potential formation of microemboli and decreased cerebral blood flow (43).

The homing and migratory ability of HSPCs in our study is perhaps unsurprising, as hematopoietic progenitors ultimately differentiate into blood cells that themselves have migratory abilities, as the machinery with which to respond to chemokine and cytokine gradients. In fact, HPSCs have previously been shown to express both vascular cell adhesion molecule-1 and its receptor very late antigen-4 (44, 45),

both of which would aid in the migratory process into the brain (46, 47). Interestingly, our findings demonstrated a vast improvement between HPSC- and saline-treated mice just 24-h after administration, suggesting that the protective mechanism of the cells was unlikely to involve direct replacement of infarcted brain tissue. In fact, it has yet to be observed in humans that any type of SCs applied as a therapy replace lost neuronal circuitry (48).

Despite many studies focusing on the clarification of which signaling molecules attract SCs and direct their migration to damaged areas, little is known regarding what HPSCs do in the brain following stroke. We have demonstrated here that transcriptome in naïve HPSCs versus those that had been transplanted and had emigrated into the brain parenchyma showed marked differences in MT transcripts, in particular MT-1. RNA-seq analyses also uncovered increases in inflammation-associated transcripts and other transcripts. Upregulation of IL-10ra mRNA, suggested the activity of anti-inflammatory IL-10 pathway, which may inhibit the homing of inflammatory cells, but not that of HPSCs. The DENN domain-related pathway included upregulation of DENN/MADD domain containing 1A (*Dennd1a*), DENN/MADD domain containing 3 (*Dennd3*), and SET binding factor 1 (*Sbf1*), which has been associated with Rab-mediated processes or regulation of MAPK (mitogen-activated protein kinases) signaling (48). The oligoadenylate synthetase-related pathway included upregulation of 2'-5' oligoadenylate synthetase 1D (*Oas1d*), 2'-5' oligoadenylate synthetase 3 (*Oas3*), and 2'-5' oligoadenylate synthetase 1H (*Oas1h*), which has been associated with innate immune response (50). The steroid hormone receptor signaling pathway included upregulation of peroxisome proliferative activated receptor γ coactivator 1β (*Ppargc1b*), RNA binding protein, fox-1 homolog 2 (*Rbfox2*), and estrogen receptor 2 (*Esr2*). Since the factors released by HPSCs are broad, we have not ruled out that these factors may also be changeable depending on the evolving microenvironment within the brain. Further experiments will shed light on this.

Although we checked the differentially expressed genes whose fold changes were more than 2-fold and *P* values were less than 0.05 in treated HSPCs compared with naïve controls (Supplemental Table 1), using a

functional clustering tool, DAVID 6.8 (NIH, https://david.ncifcrf.gov/home.jsp), we found neither pro-inflammatory nor anti-inflammatory cytokines (Supplemental Table 3).

Finally, to test whether MT-I can be used as a pharmacological strategy for the treatment of stroke, we determined its impact in our model of I/RI. MT (MTI-IV) are small, free-radical scavenging proteins, ubiquitously expressed and with both intra- and extracellular functions (51, 52). Notably, they are highly inducible, and dramatically increased transcription is observed during ischemia (53) and various pro-inflammatory mediators such as IL-6 and reactive oxygen species (54), promote growth and angiogenesis, neurogenesis and expression of anti-inflammatory cytokines (55). While few studies investigate MT activity, those that do indicate their protective effects: in one study, therapeutic effects of MT administered i.p. were observed (MT-II) in a rat model of cerebral I/R) (56). Our study upholds this trend, as we have showed that MT-I (the best studied MT along with MT-II, and the most significantly increased transcript in transplanted HSPCs) administered to stroked mice could produce neuroprotection and attenuate I/R-induced cerebrovascular injury.

In summary, our results demonstrate that administration of HSPCs leads to neuroprotection in stroke. It is likely that the mechanisms providing therapeutic benefit in this study are multidimensional. However, our findings shed light on a previously unidentified mechanism of MT-1 upregulation, through which HSPCs may modulate inflammation and augment the detrimental effects of cerebral I/R. Furthermore, this was confirmed by the administration of MT-1 which was able to successfully protect against stroke. Therefore, this study demonstrates that HPSCs are an attractive treatment option for patients with stroke, and we urge the establishment of further, larger scale clinical trials investigating their therapeutic potential.

Author contributions: H.S., S.O., F.B., I.T., and F.N.E.G designed and performed research, analyzed data and wrote the paper. S.V. performed research and wrote the paper. S.P.C. wrote the paper.

Acknowledgments

References

1. Smith, H. K., Gil, C. D., Oliani, S. M., and Gavins, F. N. (2015) Targeting formyl peptide receptor 2 reduces leukocyte-endothelial interactions in a murine model of stroke. *FASEB journal : official publication of the Federation of American Societies for Experimental Biology* **29**, 2161-2171

2. Vital, S. A., Becker, F., Holloway, P. M., Russell, J., Perretti, M., Granger, D. N., and Gavins, F. N. (2016) Formyl-Peptide Receptor 2/3/Lipoxin A4 Receptor Regulates Neutrophil-Platelet Aggregation and Attenuates Cerebral Inflammation: Impact for Therapy in Cardiovascular Disease. *Circulation* **133**, 2169-2179

3. Smith, H. K., and Gavins, F. N. (2012) The potential of stem cell therapy for stroke: is PISCES the sign? *FASEB J* **26**, 2239-2252

4. Tornero, D., Wattananit, S., Gronning Madsen, M., Koch, P., Wood, J., Tatarishvili, J., Mine, Y., Ge, R., Monni, E., Devaraju, K., Hevner, R. F., Brustle, O., Lindvall, O., and Kokaia, Z. (2013) Human induced pluripotent stem cell-derived cortical neurons integrate in stroke-injured cortex and improve functional recovery. *Brain : a journal of neurology* **136**, 3561-3577

5. Tatarishvili, J., Oki, K., Monni, E., Koch, P., Memanishvili, T., Buga, A. M., Verma, V., Popa-Wagner, A., Brustle, O., Lindvall, O., and Kokaia, Z. (2014) Human induced pluripotent stem cells improve recovery in stroke-injured aged rats. *Restorative neurology and neuroscience* **32**, 547-558

6. Honmou, O., Houkin, K., Matsunaga, T., Niitsu, Y., Ishiai, S., Onodera, R., Waxman, S. G., and Kocsis, J. D. (2011) Intravenous administration of auto serum-expanded autologous mesenchymal stem cells in stroke. *Brain : a journal of neurology* **134**, 1790-1807

7. Gutierrez-Fernandez, M., Rodriguez-Frutos, B., Ramos-Cejudo, J., Teresa Vallejo-Cremades, M., Fuentes, B., Cerdan, S., and Diez-Tejedor, E. (2013) Effects of intravenous administration of allogenic bone marrow- and adipose tissue-derived mesenchymal stem cells on functional recovery and brain repair markers in experimental ischemic stroke. *Stem cell research & therapy* **4**, 11

8. Stroemer, P., Patel, S., Hope, A., Oliveira, C., Pollock, K., and Sinden, J. (2009) The neural stem cell line CTX0E03 promotes behavioral recovery and endogenous neurogenesis after experimental stroke in a dose-dependent fashion. *Neurorehabilitation and neural repair* **23**, 895-909

9. Schwarting, S., Litwak, S., Hao, W., Bahr, M., Weise, J., and Neumann, H. (2008) Hematopoietic stem cells reduce postischemic inflammation and ameliorate ischemic brain injury. *Stroke* **39**, 2867-2875

10. Oki, K., Tatarishvili, J., Wood, J., Koch, P., Wattananit, S., Mine, Y., Monni, E., Tornero, D., Ahlenius, H., Ladewig, J., Brustle, O., Lindvall, O., and Kokaia, Z. (2012) Human-induced pluripotent stem cells form functional neurons and improve recovery after grafting in stroke-damaged brain. *Stem cells* **30**, 1120-1133

11. Banerjee, S., Bentley, P., Hamady, M., Marley, S., Davis, J., Shlebak, A., Nicholls, J., Williamson, D. A., Jensen, S. L., Gordon, M., Habib, N., and Chataway, J. (2014) Intra-Arterial Immunoselected CD34+ Stem Cells for Acute Ischemic Stroke. *Stem cells translational medicine* **3**, 1322-1330

12. Wei, X., Yang, X., Han, Z. P., Qu, F. F., Shao, L., and Shi, Y. F. (2013) Mesenchymal stem cells: a new trend for cell therapy. *Acta pharmacologica Sinica* **34**, 747-754

13. Hao, L., Zou, Z. M., Tian, H., Zhang, Y. B., Zhou, H. C., and Liu, L. (2014) Stem Cell-Based Therapies for Ischemic Stroke. *BioMed research international*

14. Horie, N., Pereira, M. P., Niizuma, K., Sun, G. H., Keren-Gill, H., Encarnacion, A., Shamloo, M., Hamilton, S. A., Jiang, K. W., Huhn, S., Palmer, T. D., Bliss, T. M., and Steinberg, G. K. (2011) Transplanted Stem Cell-Secreted Vascular Endothelial Growth Factor Effects Poststroke Recovery, Inflammation, and Vascular Repair. *Stem cells* **29**, 274-285

15. Ma, X. L., Liu, K. D., Li, F. C., Jiang, X. M., Jiang, L., and Li, H. L. (2013) Human Mesenchymal Stem Cells Increases Expression of alpha-Tubulin and Angiopoietin 1 and 2 in Focal Cerebral Ischemia and Reperfusion. *Current neurovascular research* **10**, 103-111

16. Gavins, F. N., and Smith, H. K. (2015) Cell tracking technologies for acute ischemic brain injury. *J Cereb Blood Flow Metab*

17. Smith, H. K., Russell, J. M., Granger, D. N., and Gavins, F. N. E. (2015) Critical differences between two classical surgical approaches for middle cerebral artery occlusion-induced stroke in mice. *J Neurosci Meth* **249**, 99-105

18. Chen, J., Zhang, C., Jiang, H., Li, Y., Zhang, L., Robin, A., Katakowski, M., Lu, M., and Chopp, M. (2005) Atorvastatin induction of VEGF and BDNF promotes brain plasticity after stroke in mice. *J Cereb Blood Flow Metab* **25**, 281-290

19. Li, Y., Chopp, M., Chen, J., Wang, L., Gautam, S. C., Xu, Y. X., and Zhang, Z. (2000) Intrastriatal transplantation of bone marrow nonhematopoietic cells improves functional recovery after stroke in adult mice. *J Cereb Blood Flow Metab* **20**, 1311-1319

20. Swamydas, M. and Lionakis, M.s. (2013). Isolation, purification and labeling of mouse bone marrow neutrophils for functional studies and adoptive transfer experiments. *J Vis Exp.* **77,** e50586

21. Giralt, M., Penkowa, M., Lago, N., Molinero, A., and Hidalgo, J. (2002) Metallothionein-1+2 protect the CNS after a focal brain injury. *Experimental neurology* **173**, 114-128

22. Yanagida, K., Liu, C. H., Faraco, G., Galvani, S., Smith, H. K., Burg, N., Anrather, J., Sanchez, T., Iadecola, C., and Hla, T. (2017) Size-selective opening of the blood-brain barrier by targeting endothelial sphingosine 1-phosphate receptor 1. *Proceedings of the National Academy of Sciences of the United States of America* **114**, 4531-4536

23. Mortazavi, A., Williams, B. A., McCue, K., Schaeffer, L., and Wold, B. (2008) Mapping and quantifying mammalian transcriptomes by RNA-Seq. *Nature methods* **5**, 621-628

24. Sun, J., Nishiyama, T., Shimizu, K., and Kadota, K. (2013) TCC: an R package for comparing tag count data with robust normalization strategies. *BMC bioinformatics* **14**, 219

25. Omura, S., Kawai, E., Sato, F., Martinez, N. E., Chaitanya, G. V., Rollyson, P. A., Cvek, U., Trutschl, M., Alexander, J. S., and Tsunoda, I. (2014) Bioinformatics multivariate analysis determined a set of phase-specific biomarker candidates in a novel mouse model for viral myocarditis. *Circulation. Cardiovascular genetics* **7**, 444-454

26. Jolliffe, I. T. (2011) Principal Component Analysis, Second Edition. New York: Springer. *Briefings in bioinfomatics* **12**, 65-72

27. Chaitanya, G. V., Omura, S., Sato, F., Martinez, N. E., Minagar, A., Ramanathan, M., Guttman, B. W., Zivadinov, R., Tsunoda, I., and Alexander, J. S. (2013) Inflammation induces neuro-lymphatic

protein expression in multiple sclerosis brain neurovasculature. *Journal of neuroinflammation* **10**, 125

28. Sato, F., Omura, S., Kawai, E., Martinez, N. E., Acharya, M. M., Reddy, P. C., Chaitanya, G. V., Alexander, J. S., and Tsunoda, I. (2014) Distinct kinetics of viral replication, T cell infiltration, and fibrosis in three phases of myocarditis following Theiler's virus infection. *Cellular immunology* **292**, 85-93

29. Ogawa, M., Tajima, F., Ito, T., Sato, T., Laver, J. H., and Deguchi, T. (2001) CD34 expression by murine hematopoietic stem cells. Developmental changes and kinetic alterations. *Annals of the New York Academy of Sciences* **938**, 139-145

30. Smith, H. K., Russell, J. M., Granger, D. N., and Gavins, F. N. (2015) Critical differences between two classical surgical approaches for middle cerebral artery occlusion-induced stroke in mice. *J Neurosci Methods* **249**, 99-105

31. Chung, R. S, Penkowa, M., Dittmann, J., King, C. E., Bartlett, C., Asmussen, J. W., Hidalgo, J., Carrasco, J., Leung, Y, K., Walker, A. K., Fung, S. J., Dunlop, S. A., Fitzgerald, M., Beazley, L. D., Chuah, M. I., Vickers, J. C., West, A. K. (2008) Redefining the role of metallothionein within the injured brain: extracellular metallothioneins play an important role in the astrocyte-neuron response to injury. *J Biol Chem.* **283,** 15349-15358.

32. Paczkowska, E., Larysz, B., Rzeuski, R., Karbicka, A., Jalowinski, R., Kornacewicz-Jach, Z., Ratajczak, M. Z., and Machalinski, B. (2005) Human hematopoietic stem/progenitor-enriched CD34(+) cells are mobilized into peripheral blood during stress related to ischemic stroke or acute myocardial infarction. *Eur J Haematol* **75**, 461-467

33. England, T. J., Abaei, M., Auer, D. P., Lowe, J., Jones, D. R., Sare, G., Walker, M., and Bath, P. M. (2012) Granulocyte-colony stimulating factor for mobilizing bone marrow stem cells in subacute stroke: the stem cell trial of recovery enhancement after stroke 2 randomized controlled trial. *Stroke* **43**, 405-411

34. Gavins, F. N., Hughes, E. L., Buss, N. A., Holloway, P. M., Getting, S. J., and Buckingham, J. C. (2012) Leukocyte recruitment in the brain in sepsis: involvement of the annexin 1-FPR2/ALX anti-

inflammatory system. *FASEB journal : official publication of the Federation of American Societies for Experimental Biology* **26**, 4977-4989

35. Vasconcelos-dos-Santos, A., Rosado-de-Castro, P. H., de Souza, S. A. L., Silva, J. D., Ramos, A. B., de Freitas, G. R., da Fonseca, L. M. B., Gutfilen, B., and Mendez-Otero, R. (2012) Intravenous and intra-arterial administration of bone marrow mononuclear cells after focal cerebral ischemia: Is there a difference in biodistribution and efficacy? *Stem Cell Res* **9**, 1-8

36. Taguchi, A., Soma, T., Tanaka, H., Kanda, T., Nishimura, H., Yoshikawa, H., Tsukamoto, Y., Iso, H., Fujimori, Y., Stern, D. M., Naritomi, H., and Matsuyama, T. (2004) Administration of CD34(+) cells after stroke enhances neurogenesis via angiogenesis in a mouse model. *J Clin Invest* **114**, 330-338

37. Yilmaz, G., Vital, S., Yilmaz, C. E., Stokes, K. Y., Alexander, J. S., and Granger, D. N. (2011) Selectin-mediated recruitment of bone marrow stromal cells in the postischemic cerebral microvasculature. *Stroke* **42**, 806-811

38. Prasad, K., Sharma, A., Garg, A., Mohanty, S., Bhatnagar, S., Johri, S., Singh, K. K., Nair, V., Sarkar, R. S., Gorthi, S. P., Hassan, K. M., Prabhakar, S., Marwaha, N., Khandelwal, N., Misra, U. K., Kalita, J., Nityanand, S., and Grp, I. S. (2014) Intravenous Autologous Bone Marrow Mononuclear Stem Cell Therapy for Ischemic Stroke A Multicentric, Randomized Trial. *Stroke* **45**, 3618-3624

39. Shyu, W. C., Lin, S. Z., Yang, H. I., Tzeng, Y. S., Pang, C. Y., Yen, P. S., and Li, H. (2004) Functional recovery of stroke rats induced by granulocyte colony-stimulating factor-stimulated stem cells. *Circulation* **110**, 1847-1854

40. Goldmacher, G. V., Nasser, R., Lee, D. Y., Yigit, S., Rosenwasser, R., and Iacovitti, L. (2013) Tracking Transplanted Bone Marrow Stem Cells and Their Effects in the Rat MCAO Stroke Model. *PloS one* **8**

41. Mitkari, B., Nitzsche, F., Kerkela, E., Kuptsova, K., Huttunen, J., Nystedt, J., Korhonen, M., and Jolkkonen, J. (2014) Human bone marrow mesenchymal stem/stromal cells produce efficient

localization in the brain and enhanced angiogenesis after intra-arterial delivery in rats with cerebral ischemia, but this is not translated to behavioral recovery. *Behav Brain Res* **259**, 50-59

42. Detante, O., Moisan, A., Dimastromatteo, J., Richard, M. J., Riou, L., Grillon, E., Barbier, E., Desruet, M. D., De Fraipont, F., Segebarth, C., Jaillard, A., Hommel, M., Ghezzi, C., and Remy, C. (2009) Intravenous administration of 99mTc-HMPAO-labeled human mesenchymal stem cells after stroke: in vivo imaging and biodistribution. *Cell transplantation* **18**, 1369-1379

43. Cui, L. L., Kerkela, E., Bakreen, A., Nitzsche, F., Andrzejewska, A., Nowakowski, A., Janowski, M., Walczak, P., Boltze, J., Lukomska, B., and Jolkkonen, J. (2015) The cerebral embolism evoked by intra-arterial delivery of allogeneic bone marrow mesenchymal stem cells in rats is related to cell dose and infusion velocity. *Stem cell research & therapy* **6**

44. Ulyanova, T., Scott, L. M., Priestley, G. V., Jiang, Y., Nakamoto, B., Koni, P. A., and Papayannopoulou, T. (2005) VCAM-1 expression in adult hematopoietic and nonhernatopoietic cells is controlled by tissue-inductive signals and reflects their developmental origin. *Blood* **106**, 86-94

45. Imai, Y., Shimaoka, M., and Kurokawa, M. (2010) Essential roles of VLA-4 in the hematopoietic system. *Int J Hematol* **91**, 569-575

46. Yednock, T. A., Cannon, C., Fritz, L. C., Sanchez-Madrid, F., Steinman, L., and Karin, N. (1992) Prevention of experimental autoimmune encephalomyelitis by antibodies against alpha 4 beta 1 integrin. *Nature* **356**, 63-66

47. Tsunoda, I., Terry, E. J., Marble, B. J., Lazarides, E., Woods, C., and Fujinami, R. S. (2007) Modulation of experimental autoimmune encephalomyelitis by VLA-2 blockade. *Brain pathology* **17**, 45-55

48. Janowski, M., Wagner, D. C., and Boltze, J. (2015) Stem Cell-Based Tissue Replacement After Stroke: Factual Necessity or Notorious Fiction? *Stroke*

49. Levivier, E., Goud, B., Souchet, M., Calmels, T. P., Mornon, J. P., and Callebaut, I. (2001) uDENN, DENN, and dDENN: indissociable domains in Rab and MAP kinases signaling pathways. *Biochemical and biophysical research communications* **287**, 688-695

50. Witt, P. L., Spear, G. T., Helgeson, D. O., Lindstrom, M. J., Smalley, R. V., and Borden, E. C. (1990) Basal and interferon-induced 2',5'-oligoadenylate synthetase in human monocytes, lymphocytes, and peritoneal macrophages. *Journal of interferon research* **10**, 393-402

51. Lee, S. J., and Koh, J. Y. (2010) Roles of zinc and metallothionein-3 in oxidative stress-induced lysosomal dysfunction, cell death, and autophagy in neurons and astrocytes. *Molecular brain* **3**, 30

52. Ito, Y., Tanaka, H., and Hara, H. (2013) The potential roles of metallothionein as a therapeutic target for cerebral ischemia and retinal diseases. *Current pharmaceutical biotechnology* **14**, 400-407

53. Trendelenburg, G., Prass, K., Priller, J., Kapinya, K., Polley, A., Muselmann, C., Ruscher, K., Kannbley, U., Schmitt, A. O., Castell, S., Wiegand, F., Meisel, A., Rosenthal, A., and Dirnagl, U. (2002) Serial analysis of gene expression identifies metallothionein-II as major neuroprotective gene in mouse focal cerebral ischemia. *The Journal of neuroscience : the official journal of the Society for Neuroscience* **22**, 5879-5888

54. Pedersen, M. O., Jensen, R., Pedersen, D. S., Skjolding, A. D., Hempel, C., Maretty, L., and Penkowa, M. (2009) Metallothionein-I+II in neuroprotection. *BioFactors* **35**, 315-325

55. Santos, C. R., Martinho, A., Quintela, T., and Goncalves, I. (2012) Neuroprotective and neuroregenerative properties of metallothioneins. *IUBMB life* **64**, 126-135

56. Eidizadeh, A., Khajehalichalehshtari, M., Freyer, D., and Trendelenburg, G. (2015) Assessment of the Therapeutic Potential of Metallothionein-II Application in Focal Cerebral Ischemia In Vitro and In Vivo. *PloS one* **10**, e0144035

Figure Legends

Figure 1. Overview of experimental design. Male C57BL/6J mice underwent 30 minute (min) middle cerebral artery occlusion (MCAo) followed by reperfusion. Mice were treated with hematopoietic stem/progenitor cells (HSPCs) or saline (vehicle) 24-h post-MCAo and analyses were conducted for up to 2 weeks (wk).

Figure 2. HSPCs improve outcome in the brain following I/R. Male C57BL/6J mice underwent 30-min middle cerebral artery occlusion (MCAo) followed by reperfusion. Mice were treated with hematopoietic stem/progenitor cells (HSPCs) or saline (vehicle) 24-h post-MCAo and analyses were conducted up to 2 weeks (wk). Phenotypic analysis of HSPCs cells shows consistent expression of CD34, CD31, c-kit and Sca-1, indicating HSPCs, extracted on the day of treatment to be a phenotypically stable source of cells for use as a treatment, n=5 A). Various outcome parameters were assessed throughout and at the termination of experiments in order to assess the efficacy of HSPC treatment, including mortality rates B), infarct volume C, D) for representative images, and neurological score E). $*p < 0.05$ versus sham, $^{\#}p < 0.05$ versus saline-treated mice for respective time post-MCAo; n=>6 mice per group.

Figure 3. HSPCs administered i.v. migrate to the ipsilateral hemisphere following cerebral I/R. DAB staining A-E) and sorting of CFSE-positive hematopoietic stem/progenitor cells (HSPCs) from whole brain F) indicated that HSPCs localized to the ischemic brain following cerebral I/R (graph shows ratio of HSPCs emigrated to ipsi- versus contralateral hemispheres, where the number of HSPCs in the contralateral hemisphere has been normalized to 1), and confocal intravital microscopy of the ischemic brain demonstrated that once localized, HSPCs emigrated from blood vessels into the surrounding parenchyma G). Polymorphonuclear cells (PMNs) were detected in the vessels (dotted line). No HSPCs were observed in the contralateral cortex.

Figure 4. Leukocyte-endothelial interactions in the cerebral microcirculation are reduced following HSPC treatment. Intravital microscopy was performed on mice post-MCAo A), and leukocytes visualized

using Rhodamine 6G (selectively absorbed by leukocytes) B). Marked increases in leukocyte-endothelial interactions were observed following cerebral I/R versus sham-operated animals (C and D for stills from representative videos). Videos of 3-5 venular microvessels (30-70-µm diameter) were recorded for 2-min, and then analysed with respect to the number of rolling leukocytes ($mm^{-2}min^{-1}$) E) and their velocity ($µm^{-1}min^{-1}$) F), as well as the number of leukocytes adherent to the cells wall for $\geq$30-sec ($mm^{-2}min^{-1}$) G). No interactions were observed in arterioles (data not shown). *$p < 0.05$ versus sham, #$p < 0.05$ versus saline (vehicle)-treated mice for respective time post-MCAo; n=>6 mice per group.

Figure 5. Neuroinflammation was suppressed following HSPC treatment after cerebral I/R. Activated microglia were stained (Iba-1) (A-D) and counted within three 100-µm x 100-µm cortical segments along the ipsilateral and contralateral hemispheres. The increase in activated microglia following MCAo was greater in the ipsilateral cortex, which was reduced by 50% in both cortices following HPSC treatment (E and F). *$p < 0.05$ versus saline (vehicle)-treated mice; n=4 mice per group.

Figure 6. Principal component analysis (PCA) of RNA sequencing transcriptome data from stem cells before (controls: samples C1-3, C7-9) and 24-hours after transfer ("treated": samples T4-6, T10-12). A) PCA of the 12-transcriptome data showed overall gene expression patterns. Based on the principal component (PC) 2 values, PCA separated most samples between control versus treated groups with the exception of sample T12. B) Factor loading for PC2 ranked the genes that contributed to PC2 values positively (top half. Metallothionein (*Mt*1) most significant) and negatively (bottom half). C, D) Male C57BL/6 mice underwent 30-min MCAo followed by reperfusion. Mice were treated with MT-1 or PBS (vehicle) 24-h post-MCAo and neurological score C) and infarct volume (D) were quantified.

Figure 7. Schematic overview of the important protective role HPSCs play in abrogating I/R-induced cerebrovascular injury. i.v., intravenous; I/R, ischemia/reperfusion; IV, infarct volume; NS, neurological score; MT, metallothionein.
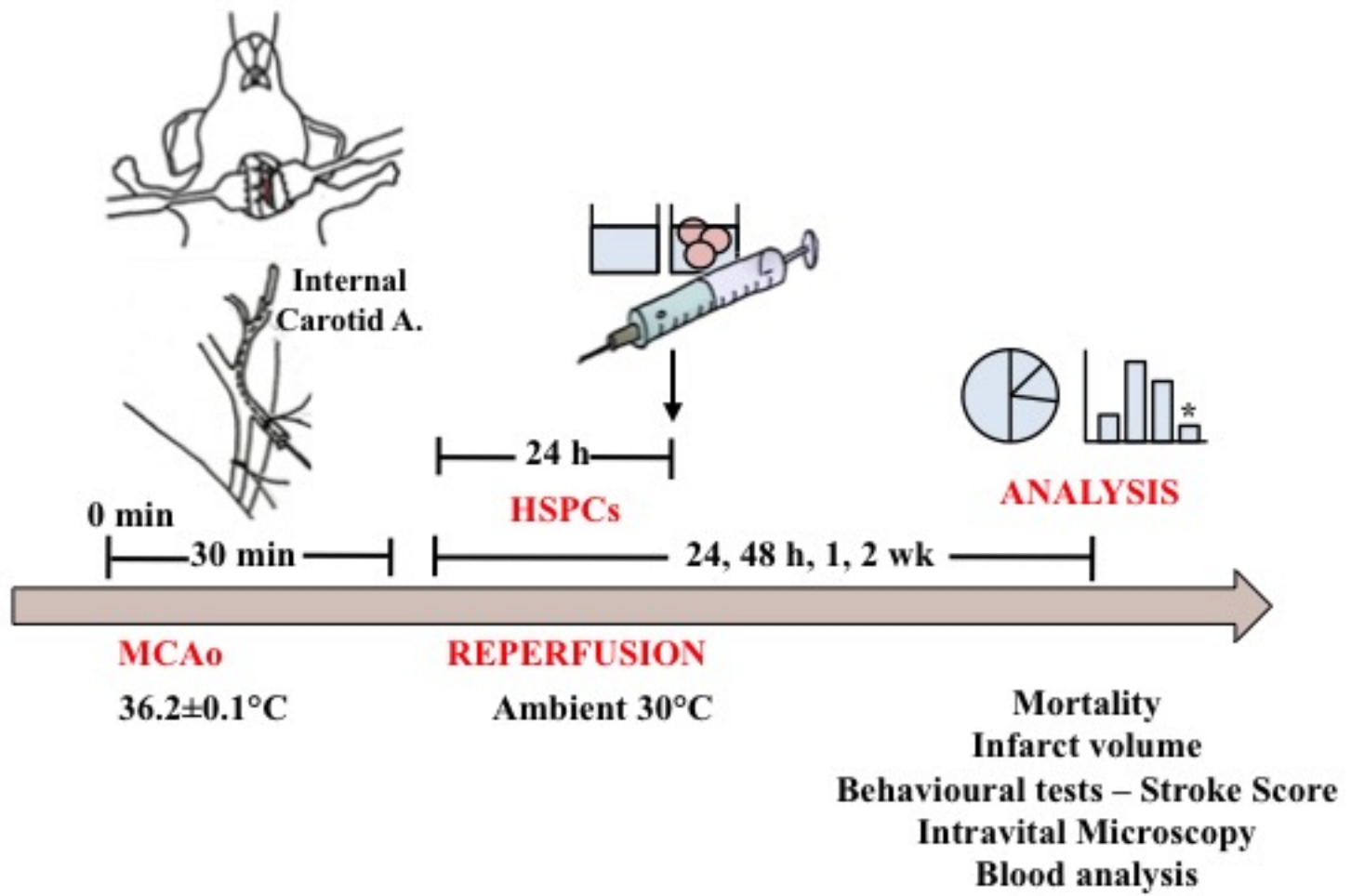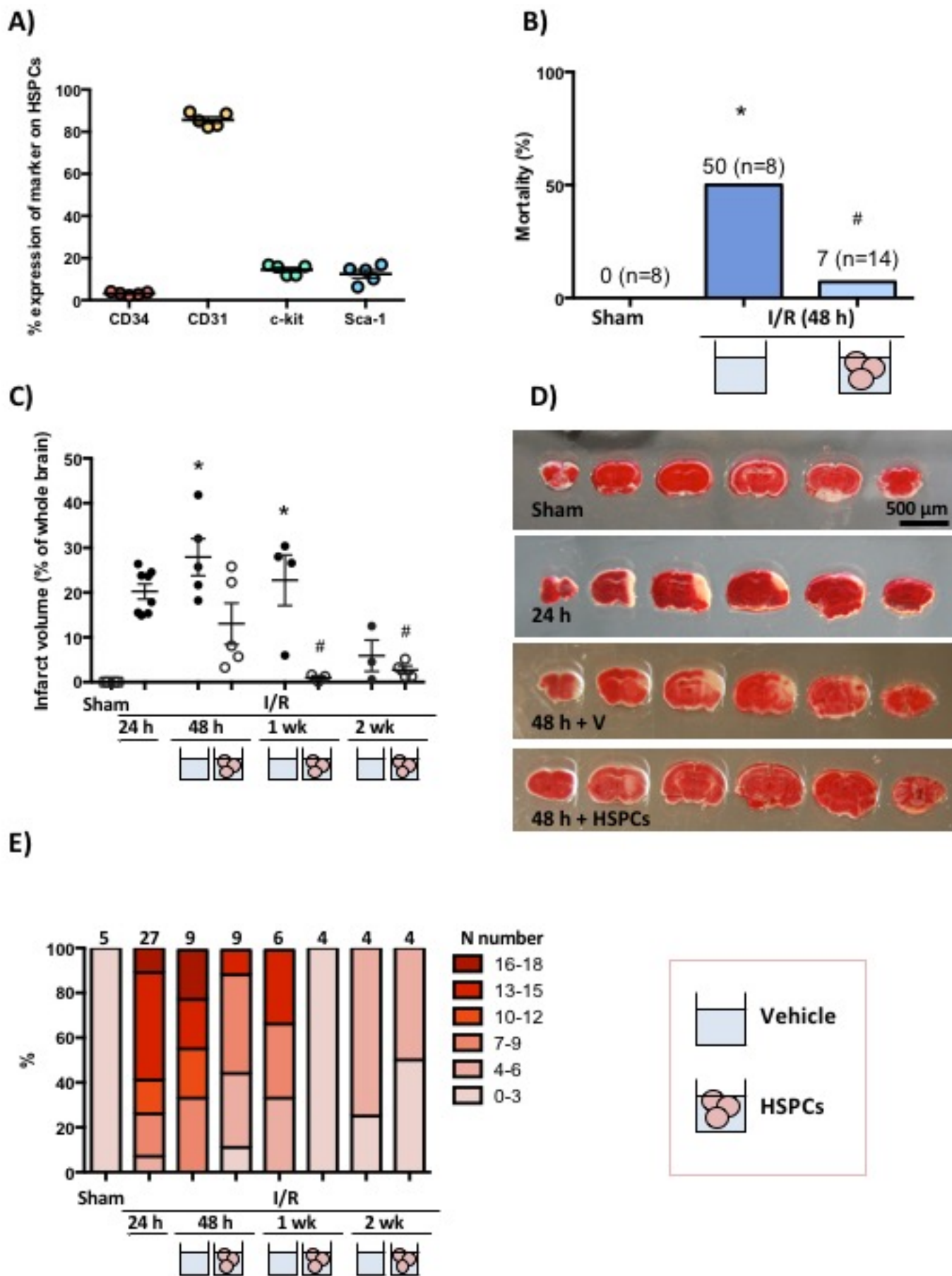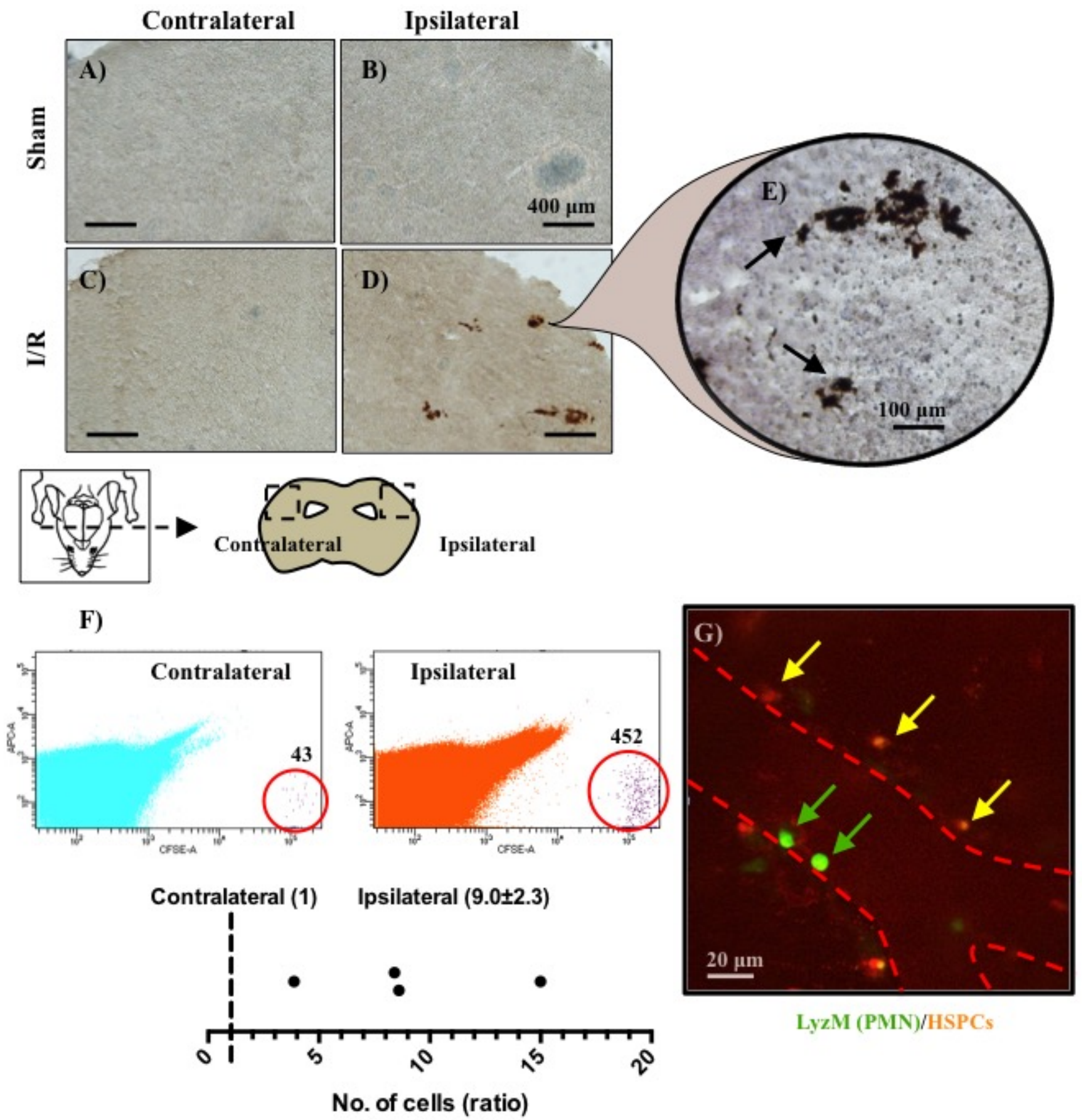
Figure 1

Figure 1

Figure 2

Figure 3

Figure 4

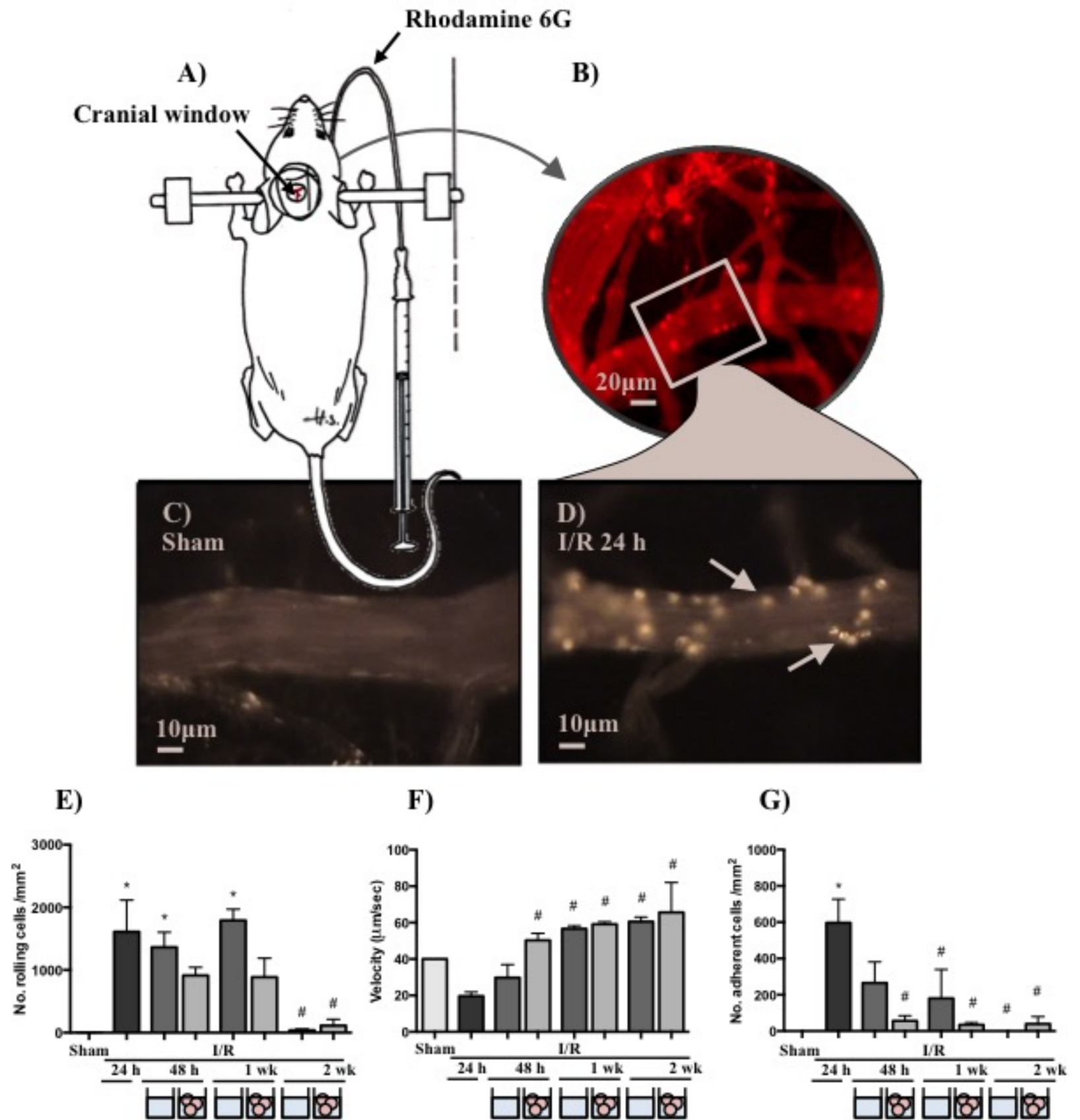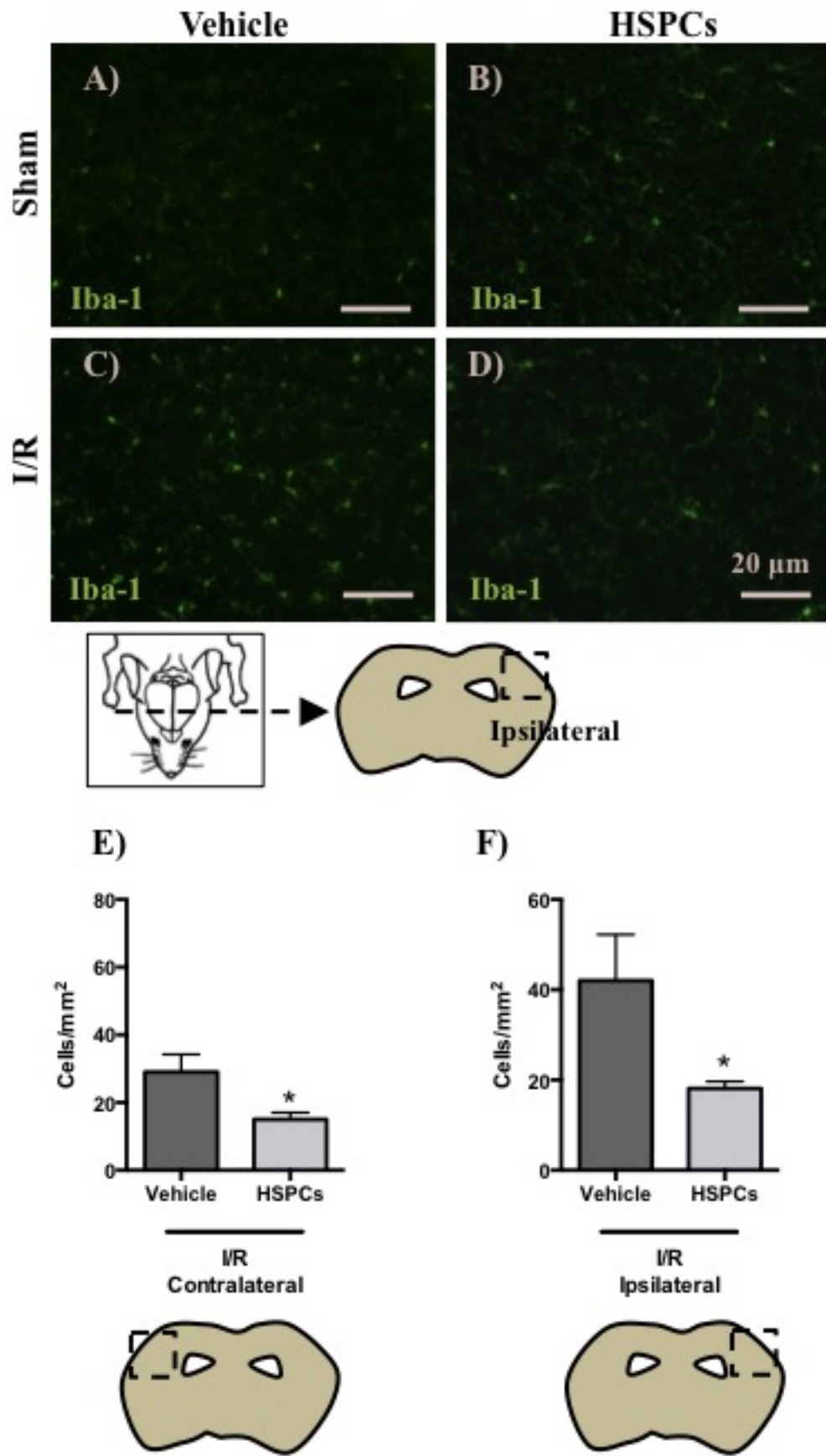Figure 4

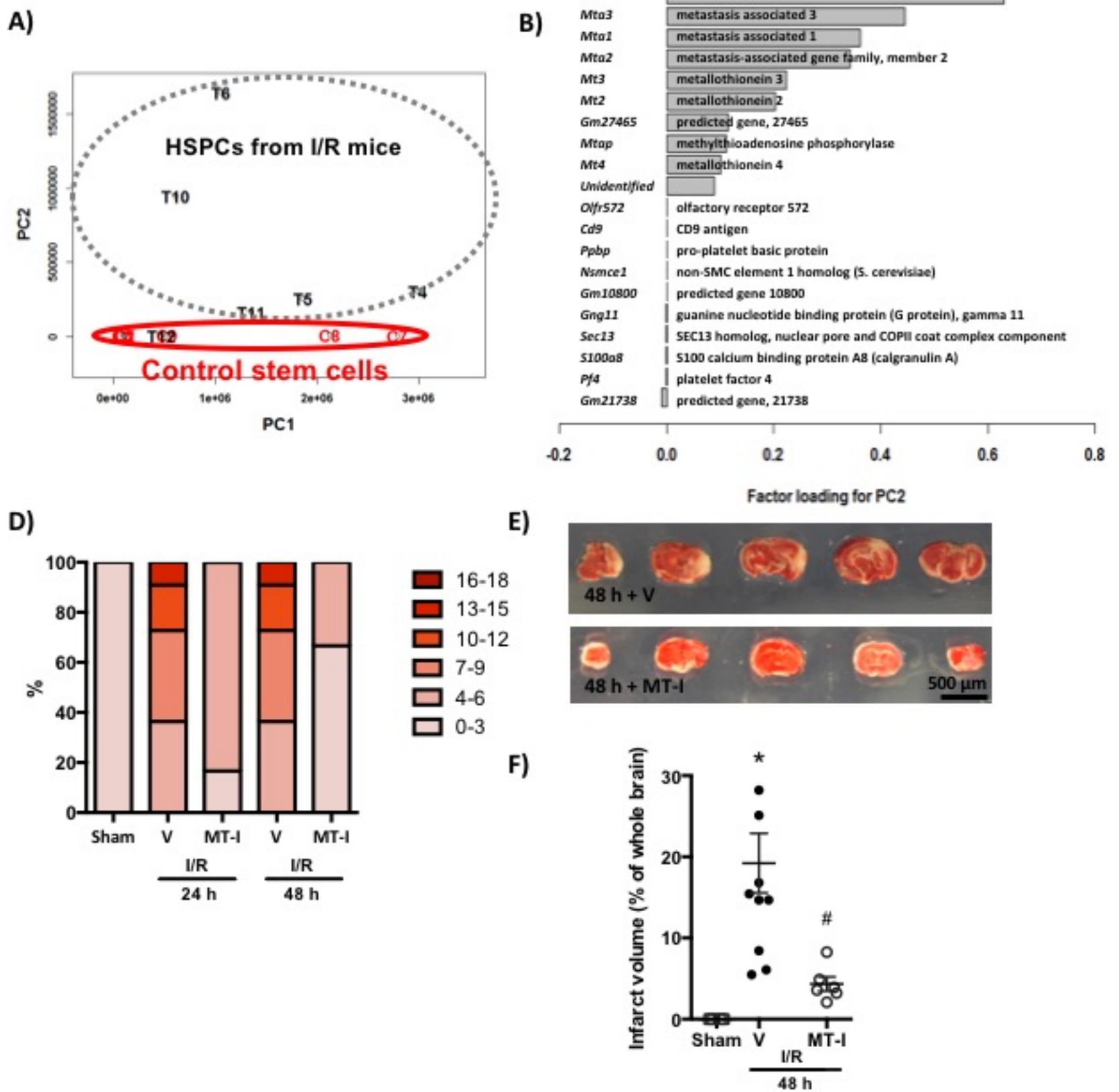# Figure 5

Figure 5
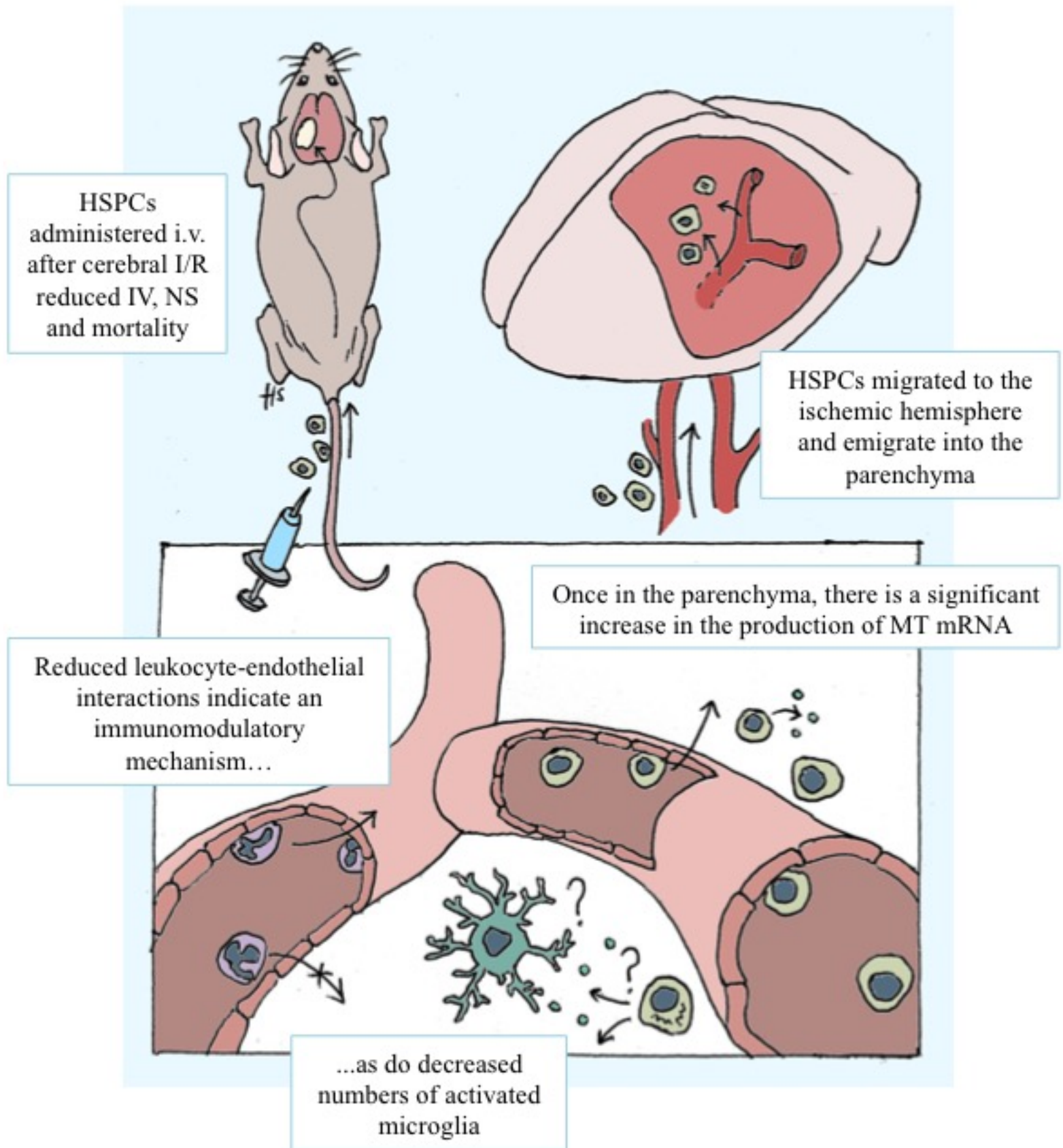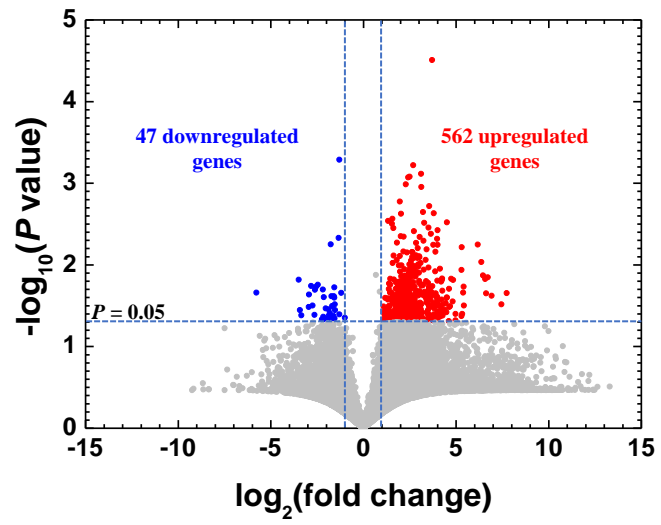
Figure 6

Figure. 6

Figure 7

Figure 7

Table 1. 18-point Neurological score (one point where any of the following apply)

Sense assessed	Test
General	Irritability/piloerection
	Immobility/staring
	Seizures/monoclonus/tremor
Motor	Flexion of forelimb
	Flexion of hindlimb
	Head tilt 10 degrees
	Some circling
	Circling over 50% of the tme while moving
	Inability to walk straight
	Falling down
Sensory	Corneal reflex
	Pinna reflex (response to pinch of ear "lobe")
	Startle reflex
Proprioception	Grasps side of beam
	Hugs beam, one limb down
	Hugs beam, two limbs down/spins about the beam
	Falls down after 5 sec attempt to balance
	No attempt to balance, falls down

SUPPLEMENTAL MATERIAL

Supplemental Figure 1

MT-1
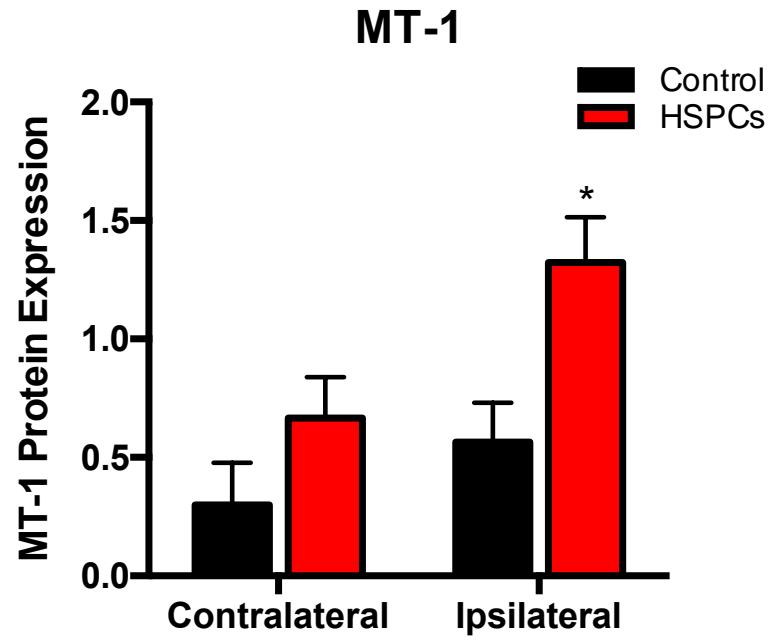
Supplemental Figure Legends

Supplemental Figure 1. Volcano plot showing transcriptome analysis of 562 genes and 47 genes that were significantly up- or downregulated more than 2-fold, respectively, in isolated versus naïve HPSCs.

Supplemental Figure 2. HSPCs increase MT-1 expression in the brain following I/R. Male C57BL/6J mice underwent 30-min middle cerebral artery occlusion (MCAo) followed by reperfusion. Mice were treated with hematopoietic stem/progenitor cells (HSPCs) or saline (vehicle) 24-h post-MCAo and 24-h later brains were harvested and separated into ipsilateral (Ips) and contralateral (Cont) regions. Blots were stained for MT-1 and then stripped and stained for tubulin to monitor protein loading. Densitometric analysis of MT-1. Values in B are means ± SE of n = 4 mice/group. *$p < 0.05$ vs. vehicle ipsilateral.

Supplemental Table 1.

Read count data of all genes (total 38924 genes) in naïve HPSCs (Naïve SC1, 2, 3, 7, 8, and 9) and treated HPSCs (Treated SC4, 5, 6, 10, 11, and 12). Exon read count data of 12 samples given were normalized with two methods: 1) read counts per kilobase (RPK) and 2) tag count comparison (TCC), using "R". Fold changes were calculated using the average read count data of 6 naïve HPSCs data divided by those of 6 treated HPSCs. p values were calculated by Student's t-test between naïve and treated HPSC groups. Data were sorted by p values and fold changes.

Supplemental Table 2.

Read count data of inflammatory and angiogenic factor genes in naïve and treated HPSCs. Interleukin-10 receptor α subunit (*Il10ra*) and epiregulin (*Ereg*) were significantly upregulated (*Il10ra*: 4.2-fold, $p<0.05$; *Ereg*: 6.9-fold, $p<0.05$).

Supplemental Table 3.

Functional clustering of significantly up- or down-regulated genes based on analyses of gene expression data of Supplemental Table 1 by the Database for Annotation Visualization and Integrated Discovery (DAVID). The list of genes up- or down-regulated in treated HPSCs ($p<0.05$, more than 2-fold up- or down-regulated between the control and treated groups) was uploaded into DAVID for functional clustering. Enrichment score was calculated by Fisher's Exact Test based on the number of differentially expressed genes in the sample as well as

the total number of genes that were included in each canonical pathway in the database. Among the pathways, the DENN (after differentially expressed in neoplastic versus normal cells) domain-related pathway (Cluster 1), oligoadenylate synthetase-related pathway (Cluster 2), and steroid hormone receptor signalling pathway (Cluster 3) were listed as top three pathways based on enrichment scores.